



# Volcano Seismology: Detecting Unrest in Wiggly Lines

R.O. Salvage, S. Karl and J.W. Neuberg

## Abstract

Seismology is a useful tool to gain a better understanding of volcanic unrest in real time as it unfolds. The generation of seismic signals in a volcanic environment has been linked to a number of different physical processes occurring at depth, including fracturing of the volcanic edifice (producing high frequency seismicity) and movement of magmatic fluids (producing low frequency seismicity). Further classification of seismic signals according to their waveform similarity, in addition to their frequency content, allows greater detail in temporal and spatial changes of seismicity to be detected. At Soufrière Hills volcano, Montserrat, one of the target volcanoes of the VUELCO project, families of similar waveforms provided valuable insight into evaluating the significance of ongoing unrest. In June 1997 over 6000 more events were able to be identified over a 5 day period of interest (22 to 25 June) by using families of seismic events, rather than a standard amplitude-based detection algorithm. In total, 11 families were identified, with the events clustering into a number of swarms, suggesting a repeating and non destructive cyclic source mechanism. Since each family is believed to represent a distinct source location and mechanism, identifying 11 coexisting families

---

R.O. Salvage (✉)  
Observatorio Vulcanológico y Sismológico  
de Costa Rica, Universidad Nacional,  
Apartado Postal: 2386-3000, Heredia, Costa Rica  
e-mail: [beckysalvage@gmail.com](mailto:beckysalvage@gmail.com)

S. Karl  
Shell, NAM offices, Schepersmaat 2,  
9405 TA Assen, The Netherlands  
e-mail: [sandra.karl84@gmail.com](mailto:sandra.karl84@gmail.com)

J.W. Neuberg  
School of Earth and Environment, Institute of  
Geophysics and Tectonics, University of Leeds,  
Leeds LS2 9JT, United Kingdom  
e-mail: [j.neuberg@leeds.ac.uk](mailto:j.neuberg@leeds.ac.uk)

reflects the complex diversity of physical processes which act simultaneously at this volcano. In July 2003, conditions at the volcano had clearly changed since only one family of seismicity was identified. The source location of this family appeared to shift with time from 8 July (when no events from the family were identified) to 12 July (where most events had a cross correlation coefficient over 0.9). In addition, the use of families appears to greatly aid hindsight forecasting attempts for the large scale dome collapses of 1997 and 2003 using the Failure Forecast Method. Knowledge of the temporal and spatial extent of seismicity during periods of unrest, its source mechanism and its relationship to physical processes at depth is essential for decision and policy makers for risk mitigation. However, the source mechanisms of such volcanic seismicity is still much debated and appears to often be misinterpreted because of compromising assumptions used in the numerical modelling of inverting such sources. Use of a spatially extended source such as a ring fault structure, rather than a single point for determining the origin of low frequency seismicity, is now thought to be more realistic for the mechanism of such events since it more accurately represents the movement of magma through a conduit. However, use of this spatially extended source instead of a simple single point results in a large underestimation of slip from P-wave amplitudes, which may lead to an underestimation in magma ascent rates, with large consequences for eruption forecasting. Additionally, the P-wave radiation patterns exhibited by these two mechanisms are remarkably similar, and can only be distinguished if the small radial radiation lobes can be determined. In a volcanic environment this is extremely difficult due to large uncertainties in earthquake source depth locations, and the implementation of small aperture seismic networks.

---

### **Español**

La sismología es una herramienta geofísica valiosa que brinda información en tiempo real, permitiendo una mejor comprensión del comportamiento de sistemas volcánicos que inician un proceso de reactivación o de intensificación de la actividad. La generación de señales sísmicas en ambientes volcánicos se ha relacionado con un número diverso de procesos geofísicos que ocurren en el interior de los volcanes, incluyendo fracturamiento del edificio volcánico (produciéndose sismicidad de alta frecuencia) y movimiento de fluidos magmáticos (produciéndose sismicidad de baja frecuencia). La clasificación de señales sísmicas basada en la similitud de las formas de onda, además del contenido de frecuencias, ha permitido detectar cambios temporales y espaciales de la sismicidad con mayor detalle.

En el volcán Soufriere Hills en Monserrat, uno de los volcanes investigados como parte del Proyecto VUELCO, el reconocimiento de familias de señales sísmicas con formas de onda similares proveyó un entendimiento valioso en la evaluación de la significancia de la

reactivación de su actividad volcánica. En junio de 1997, se pudieron identificar más de 6000 eventos sísmicos dentro de un periodo particular de 4 días (entre el 22 y el 25 de junio) mediante la determinación de familias de eventos sísmicos que fueron determinados por un algoritmo estándar de detección basado en la amplitud de la señal sísmica. En total, 11 familias de eventos sísmicos fueron identificadas, con grupos de eventos conformando enjambres sísmicos, lo que sugiere un mecanismo cíclico repetitivo de una fuente sísmica no destructiva. Ya que se considera que cada familia representa una fuente con ubicación espacial y mecanismo distinto, la identificación de 11 familias refleja la compleja diversidad de los procesos geofísicos que operan simultáneamente en este volcán en particular. En julio del 2003, el régimen del volcán cambió definitivamente ya que solamente 1 familia de eventos sísmicos fue identificada. La ubicación de la fuente sísmica de esta familia parece haber migrado con el tiempo entre el 8 de julio (cuando ningún evento sísmico de esta familia fue identificado) y el 12 de julio (cuando la mayoría de eventos tuvo un coeficiente de cros-correlación superior a 0,9). Además, el establecimiento de familias de sismos parece haber sido de gran ayuda en los intentos de pronosticar los colapsos del domo en gran escala de 1997 y el 2003 utilizando el método determinístico de pronóstico de rompimiento por fatiga (Failure Forecast Method, FFM). El conocimiento de la extensión temporal y espacial de la sismicidad durante periodos de reactivación volcánica, el mecanismo de la fuente, y su relación con los procesos geofísicos a niveles profundos son aspectos esenciales para los tomadores de decisiones y ejecutores de políticas relacionadas con la mitigación de riesgos.

En general, los mecanismos de la fuente generadora de la sismicidad volcánica continúan aún bajo gran debate y parecen ser con frecuencia mal interpretados debido a simplificaciones comprometedoras usadas en los modelos numéricos de inversión de dichas fuentes. El uso de una fuente espacial extendida tal como una falla estructural tipo anular, en lugar de un solo punto para determinar el origen de sismicidad de baja frecuencia, se piensa es más realista para visualizar el mecanismo de este tipo de eventos ya que representa con más exactitud el movimiento del magma a través de un conducto. Sin embargo, el uso de este modelo resulta en la subestimación significativa del deslizamiento en la falla determinada a través de las amplitudes de las ondas P, lo que podría llevar a una subestimación de las tasas de ascenso del magma, con consecuencias cruciales para el pronóstico de erupción inminente. Por otra parte, los patrones de radiación de la onda P mostrados por estos dos mecanismos son marcadamente similares, y pueden ser solamente distinguidos si los pequeños lóbulos radiales de radiación pueden ser determinados. En un contexto volcánico, esta es una tarea extremadamente difícil debido a la gran incertidumbre inherente a la localización de la profundidad de la fuente sísmica, y a la implementación de redes sísmicas de pequeña extensión.

**Keywords**

Volcano seismology · Families of similar seismic events · Magmatic source mechanism · Eruption forecasting

**Index Terms**

Volcano seismology · Soufrière Hills · Chiles-Cerro Negro · Low frequency seismicity · Families · Cross correlation · Forecasting · Failure forecast method · Source mechanisms · Point source · CLVD · Ring fault · Spatially extended source · P-wave radiation patterns

---

**Volcanic Unrest**

The monitoring of active volcanoes for the protection of society has excelled in recent decades fuelled by rapid technological advances, which have allowed the development and deployment of more cost-effective monitoring solutions. It is now possible to detect geophysical and geochemical signals from a volcano which previously would have been below the detection threshold. The routine monitoring of volcanoes during periods of quiescence is crucial, although not always feasible, in order to assess background levels of activity at volcanoes, and thus more rapidly detect the onset of future unrest. Most simply, volcanic unrest is defined as a deviation from background levels of activity towards a level which is a cause for concern over short time scales of hours to days. Volcanic unrest does not necessarily lead to eruption, although this is the most likely outcome, with 64% of 228 volcanoes that have experienced unrest since the year 2000 culminating in eruptive events (Phillipson et al. 2013).

Current monitoring efforts at volcanoes can be grouped into three categories: measurements of surface degassing; deformation; and seismic activity, which are all thought to result from the movement of magmatic fluids at depth, and therefore may provide key insights into an impending eruption. Unrest must be detected on short timescales which is appropriate for decision-making, and therefore seismicity has remained a primary monitoring tool, as it can be

remotely analysed in real-time, often by an automated system, if a number of sensors are placed around the volcano. Deviation from the background level is also often easier to determine for seismicity than for other signals.

---

**Seismic Event Characterisation**

A wide variety of seismic signals exist within volcanic settings, associated with magmatic and hydrothermal fluid movement at depth, pressurization of the volcanic edifice, and/or the surface manifestation of the interaction of these processes. The variety of signals is a reflection of the number of different processes and the great structural heterogeneities found within this context. The characterisation of seismicity can be based upon waveform similarities, but is traditionally based upon the signals' time and frequency characteristics: different bands of frequency relate to different active source processes at depth, which can then be distinguished from one another, although the frequency bands associated with each process may overlap (Lahr et al. 1994).

The identification of seismic events in volcanic settings can assist with the detection of the onset and cessation of unrest, while the spatial and temporal patterns of occurrence may be informative of magma movement and changes in stress at depth, as well as the spatial extent of concern. An understanding of the physical processes occurring at depth is essential if accurate

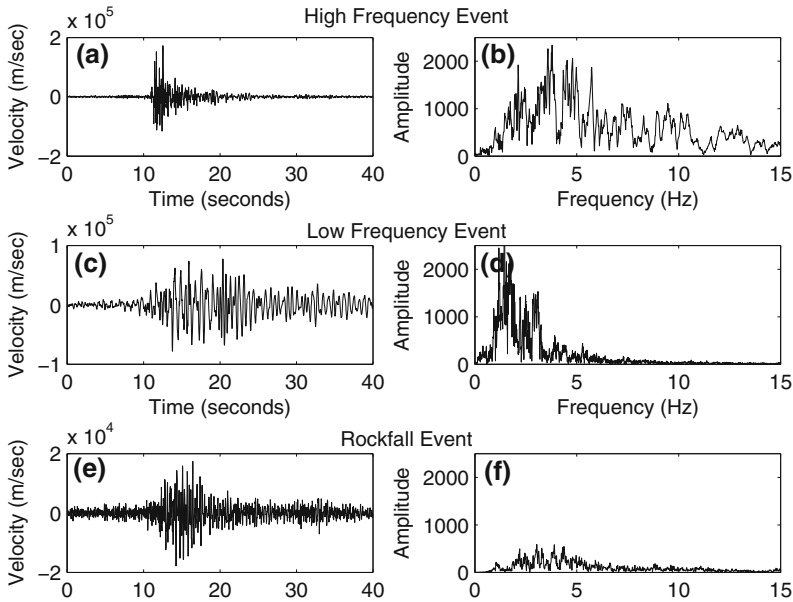


**Fig. 1** Examples of waveforms and their frequency content seen in volcanic environments taken from Soufrière Hills Volcano, Montserrat in 1997. Soufrière Hills Volcano was a target volcano identified by the VUELCO project for investigation. **a, b** High frequency

waveform with clear phase arrivals. **c, d** Low frequency waveforms with an emergent onset. Waveform filtered between 0.5 and 5 Hz. **e, f** Rockfall event with classic “cigar” shape

and timely forecasts of volcanic eruptions, and developing unrest scenarios, are to be made.

### Classification by Frequency Content

Seismic signals originating from processes occurring at depth within the volcanic system are usually split into high- and low-frequency end-members, although in reality a continuum across the spectrum exists between the two (Chouet and Matoza 2013). High frequency seismic signals (Fig. 1a, b), also known as Volcano-Tectonic (VT) events, have energy concentrated in the frequency range of 1 to 20 Hz, generally peaking between 6 and 8 Hz (Lahr et al. 1994). They are characterized by clear, impulsive P- and S-wave arrivals, followed by a short coda. High frequency seismicity is usually attributed to brittle failure within the volcanic edifice, where magmatic processes create enough elastic strain to force the surrounding rocks into failure (Arciniega-Ceballos et al.

2003), similar to the generation of tectonic earthquakes.

Low frequency (LF) seismic signals (Fig. 1c, d) usually occupy the spectral range of 0.2 to 5 Hz (Chouet and Matoza 2013), and are frequently characterized by emergent P-wave onsets and lack of S-wave arrivals. It has been suggested that the occurrence of low frequency waveforms is linked to resonance of seismic energy trapped at a solid-fluid interface either within a crack (e.g. Chouet 1988), or a volcanic conduit (e.g. Neuberg et al. 2000). The trigger mechanism of such seismic energy is further disputed, with suggestions that it may be generated by: (1) a stick-slip motion along the conduit walls as magma ascends (e.g. Iverson et al. 2006); (2) the brittle failure of magma itself either through an increase in viscosity and strain rates (Lavallée et al. 2008), which may be due to an increase in the ascent rate of magma through the conduit (Neuberg et al. 2006), changes in the crystal and/or bubble concentration in the magma (Goto 1999), or through a change in the

geometry of the conduit (Thomas and Neuberg 2012); (3) the interaction between the magmatic and hydrothermal system at depth (e.g. Nakano and Kumagai 2005); or (4) through slow rupture and failure of unconsolidated material on volcanic slopes (Bean et al. 2014).

Many volcanic seismic events fall between these two end-member categories and are termed “hybrid” events. Hybrid events are characterised by a high frequency onset with a long resonating low frequency coda, therefore distributing energy across a wider frequency spectrum (Chouet and Matoza 2013). Hybrid and LF events are often classified in the same group of volcanic seismicity, since source and path effects can result in a LF event recorded at one station being recorded as a hybrid event at another.

With the deployment of broadband sensors in many volcanic environments, it is now possible to detect seismicity within a much wider frequency band, up to 120 s periods (Chouet and Matoza 2013), known as Very Long Period (VLP) earthquakes. VLP events occupy the spectral range below 0.01 Hz. The generation of these waveforms is not yet fully understood, in particular how such long wavelengths can be generated in apparently small source volumes, although it has been linked to perturbations in the flow of fluid or gas within pressurized volcanic conduits or cracks (e.g. Dawson et al. 2011). Their large wavelength, sometimes over one hundred kilometers, means few path effects on the waveform and as such if identified, these waveforms provide an excellent choice for performing waveform inversion techniques to identify source characteristics (Chouet and Matoza 2013).

Furthermore, seismicity can be generated by surface processes, such as landslides, rockfall events, pyroclastic flows and lahars (Fig. 1e, f). These are particularly dominant during dome building eruptions and at volcanoes with glaciers during the spring and summer months due to partial melting of the ice (McNutt 2005). These signals can be exploited to determine the size and magnitude of such events, their location and their direction of travel (e.g. De Angelis et al. 2007). Typically rockfall events (small free falling rock

events) form a “cigar shaped” waveform with an emergent onset (Fig. 1e, f), whereby there is an initial increasing amplitude of the waveform as the amount of material falling down slope increases. Pyroclastic flow signals are distinguishable from rockfalls since their waveforms are at least an order of magnitude larger and they often occur over a longer duration since larger amounts of material are involved moving down slope (De Angelis et al. 2007), however the two are likely to exist on a continuum.

### Classification by Waveform Similarity

Seismic waveforms can also be classified according to their similarity with other detected seismic events. The frequency content of seismic waveforms is indicative of the active processes that may be occurring within the volcanic environment and the source mechanism involved in the generation of such seismicity. The further classification of seismic events into families which all have a similar waveform shape, as well as the same frequency content, allows the depiction of temporal and spatial changes in the source mechanism and the source location on a much smaller scale (e.g. Thelen et al. 2011; Salvage and Neuberg 2016). For example, the relative relocation of families of similar seismic events at Soufrière Hills volcano, Montserrat has produced very precise source locations (e.g. De Angelis and Henton 2011). By definition, families of seismic events must be generated by the same mechanism and at the same location in order for the detected waveforms to have the same shape at the seismometer, and therefore changes in either of these parameters affect the similarity of waveforms. In many instances it is assumed that families of seismic events are generated by the same mechanism and within a similar source location, estimated at between one quarter and one tenth of the wavelength (Geller and Mueller 1980; Neuberg et al. 2006).

Waveform similarity in terms of shape and duration can be evaluated by cross correlation. Identical signals will result in a cross correlation coefficient of 1 or  $-1$ , dependent upon their

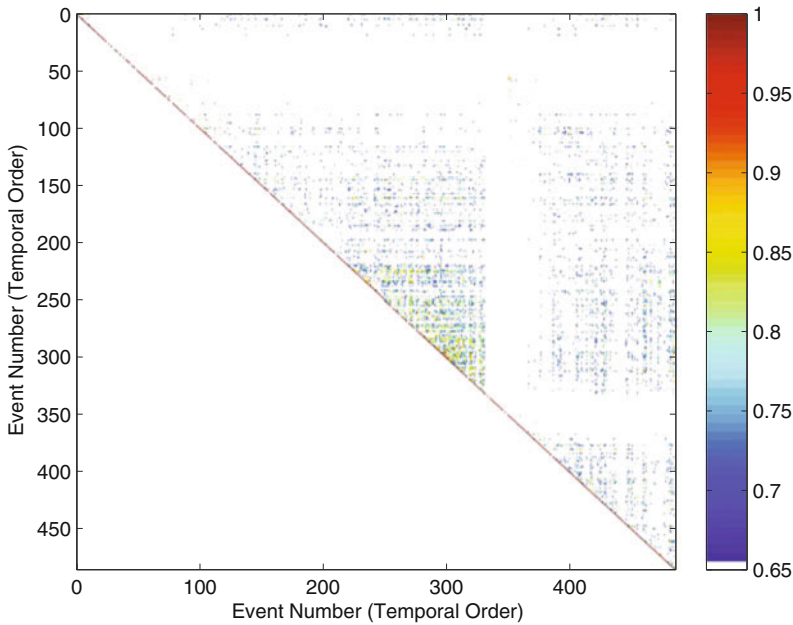


**Fig. 2** Cross Correlation Matrix of events identified at Soufrière Hills volcano, Montserrat at a single station in June 1997. A total of 486 events were identified on 24 June 1997 and are shown in temporal order along the x and y axis. Events with a cross correlation coefficient of

greater than 0.7 are shown on a colour scale, with those close to one being more similar. The autocorrelation of each event with itself is shown in *dark red* along the diagonal and is equal to a cross correlation coefficient of 1

relative polarity. Signals with no correlation result in a cross correlation coefficient of 0. A threshold must be chosen above which waveforms can be considered similar. Waveforms which are deemed similar can be grouped together into a family of events. The choice of similarity threshold is important: if it is too low there is a risk of placing events which are not similar into the same family; if it is too high similar events can be missed. Green and Neuberg (2006), Thelen et al. (2011) and Salvage and Neuberg (2016) suggest a cross correlation coefficient threshold of 0.7, since this is significantly above the correlation coefficient that can be produced from random correlations between noise and a waveform. Higher cross correlation coefficient thresholds can be used to identify families of almost identical waveforms, however Petersen (2007) suggests that this is probably not appropriate in volcanic settings due to additional noise in this environment.

The similarity between identified seismic events can be determined by cross correlating

each individual seismic event with every other seismic event. The result are typically presented as a similarity matrix, as seen in Fig. 2, where events which are deemed to be similar are shown on the colour spectrum. However, such a matrix may include a number of families of similar events since it only determines whether each event shows similarity to any of the other earthquakes analysed. In order to identify families of similar events, events with a high cross correlation coefficient as decided by the user are grouped together and removed from the matrix. This procedure is repeated across the entire investigated time period until all events have been classified into a family, or have been removed from the matrix. A master event is then determined from each family of events as the average of the stack of similar waveforms. This is representative of the family in terms of waveform shape.

Families of similar seismicity have been identified at a number of active volcanoes around the world, including Redoubt volcano, Alaska

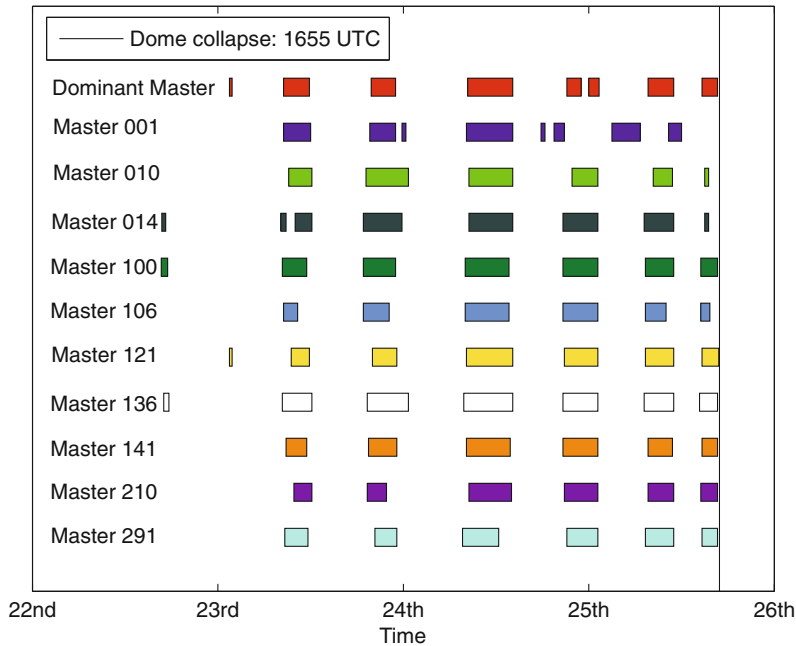


**Fig. 3** Comparison of the timing and duration of swarms of families of events identified at a single station at Soufrière Hills volcano, Montserrat in June 1997. The timing of the dome collapse is represented by the vertical line on the 25 June 1997. The y axis is only an indication of each of the families present separated in space for the

purpose of clarity on the plot and does not represent time or dominance; each master event is simply drawn below the last so that all can be compared. Each coloured *rectangular box* represents the times when the families were active during the 22–25 June analysis period

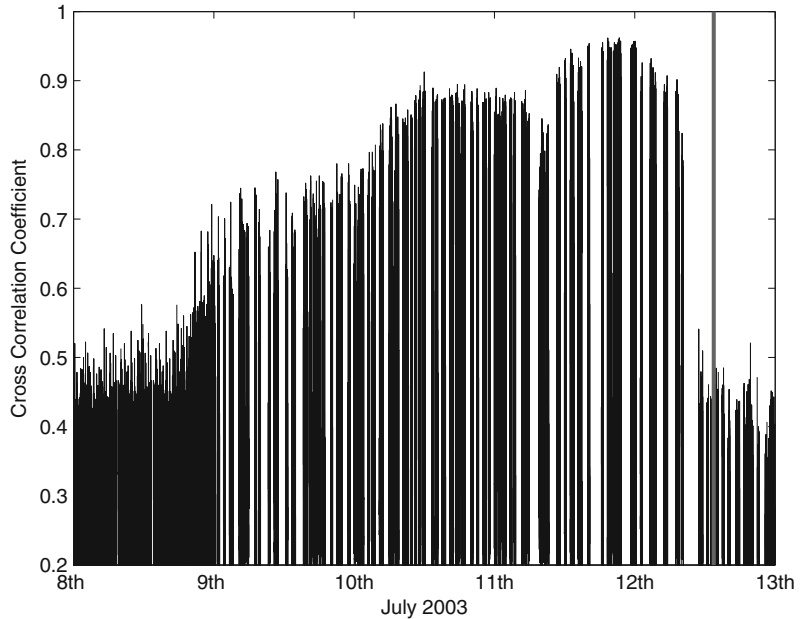
(e.g. Buurman et al. 2013); Mt. St. Helens, USA (Thelen et al. 2011); Colima, Mexico (Arámbula-Mendoza et al. 2011); Merapi, Indonesia (Budi-Santoso and Lesage 2016); Katla, Iceland (Sgattoni et al. 2016); and Soufrière Hills volcano, Montserrat (Green and Neuberg 2006; Ottemöller 2008; Salvage and Neuberg 2016). The identification of families rather than simply detecting seismic events and classifying them according to their frequency content is advantageous as subtle temporal and spatial patterns can be identified, allowing detailed source information to be uncovered. In addition, this technique dramatically increases the number of identified events from the continuous seismic record, since low amplitude events and closely spaced events can still be identified. For example, using a standard amplitude-based detection algorithm, 1435 seismic events were identified at Soufrière Hills volcano, Montserrat between 22 and 25 June 1997, a period of interest due to increased seismicity

before a lava dome collapse. The cross correlation technique identified 7653 similar seismic events during the same time period, offering a five-fold increase in the number of detected earthquakes (Salvage and Neuberg 2016).

Low frequency families of seismicity identified during this unrest period at Soufrière Hills volcano were followed by a dome collapse on 25 June 1997. Soufrière Hills Volcano was chosen by the VUELCO project as a target volcano due to the longevity of its dome building and collapse cycles which have been ongoing since 1995, providing a wealth of associated geophysical data (Sparks and Young 2002; Wadge et al. 2014). In total, 11 distinct seismic sources (i.e. 11 families of seismicity) were identified during this period of unrest [Fig. 3; Green and Neuberg (2006); Salvage and Neuberg (2016)], which all broadly follow the same temporal pattern in the number of identified swarms present over this time period. However, the timing and duration of these



**Fig. 4** The evolution of the dominant cross correlation coefficient with time at Soufrière Hills volcano, Montserrat in July 2003. A dome collapse event occurred at the time of the vertical line (13:30 on 12 July 2003). The temporal gaps in the data represent drops in the seismometer recordings rather than a change in the cross correlation coefficient, indicated by the white space on the x-axis



swarms can be seen to be different for each family of similar seismic events. Low frequency seismicity is associated with the movement of magmatic fluid at depth, and therefore in this case would suggest cyclic flow dynamics to generate such swarm-like behaviour. The source process for the generation of this seismicity must be stable and non-destructive in order to be repeatable (Green and Neuberg 2006; Petersen 2007), and must be able to occur at a number of different locations and/or by a number of different sources at the same time in order to generate a number of active families of events, reflecting the complex diversity of seismic sources and physical processes which act simultaneously at this volcano.

The identification of families can also be used to understand evolving seismicity with time. An evolving cross correlation coefficient with time, if not an artefact of data processing, may be indicative of a migrating source location or source mechanism. This was observed at Soufrière Hills volcano, Montserrat in July 2003 (Fig. 4; Salvage and Neuberg (2016)). The largest dome collapse to date observed at this volcano occurred on 12 July 2003, with removal of  $210 \times 10^6 \text{ m}^3$  of material (Herd et al. 2005), following a 4 day period from 8 to 12 July 2003

of heightened seismicity at Soufrière Hills. A migrating source mechanism can be identified from changing amplitudes in seismic events within the same family, however this characteristic cannot be identified from analysing cross correlation coefficients alone. The amplitudes of seismic events within the single family identified in July 2003 were relatively constant (Ottemöller 2008), suggesting the changing cross correlation coefficient is a consequence of a migrating source location at depth, rather than an evolving source mechanism. The generation of families ceased immediately prior to the dome collapse event, and no similar earthquakes were detected after the collapse (Fig. 4). This suggests that the physical conditions required for the generation of families were not met in the hours before, and after, the collapse event.

The analysis of families of seismicity in the time domain may also allow for the identification of spatial patterns in seismicity. Families detected at Chiles-Cerro Negro, a volcano within the Northern Andes on the border between Ecuador and Colombia in October 2014, suggests distinct temporal and spatial patterns of seismicity. The last eruption of the volcanic complex of Chiles-Cerro Negro is believed to have been

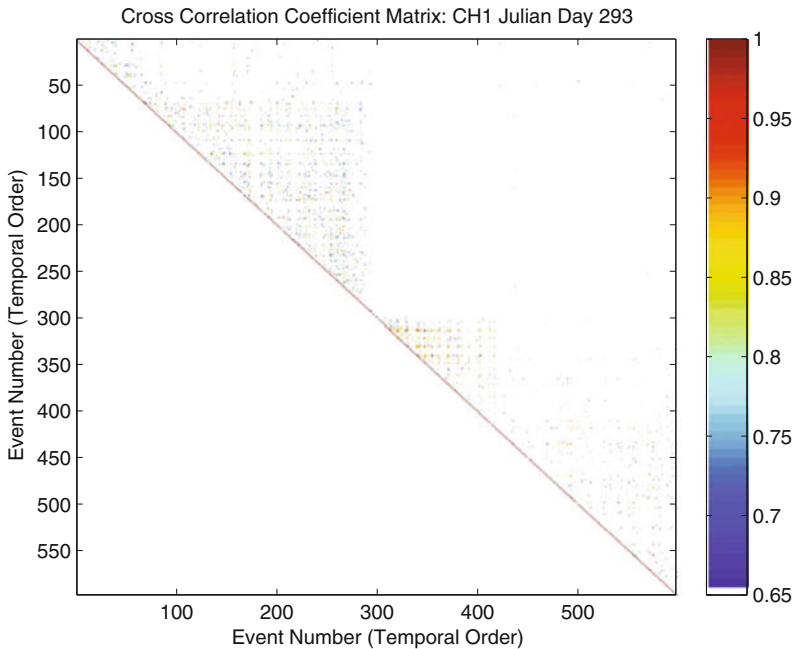


**Fig. 5** Cross Correlation Matrix of events identified using a simple amplitude based detection algorithm at Chiles-Cerro Negro on 20 October 2014, at a single station. A total of 597 events were identified and are shown in temporal order along the x and y axis. Events with a cross correlation coefficient of greater than 0.7 are shown on a colour scale, with those close to one (*red*)

being more similar. The autocorrelation of each event with itself is shown in dark red along the diagonal and is equal to a cross correlation coefficient of 1. Distinct clusters of similar events can be identified, thought to suggest a temporal evolution in the dominant similar seismicity

3400 years ago, although seismicity has since been detected in the area, thought to be related to an active hydrothermal system (Ruiz et al. 2013). The volcanic complex is dissected by a large fault system, believed to have been active as recently as 1868, when two large seismic events occurred (Mw 6.6 and 7.2) (Beauval et al. 2010). Seismic activity increased in 1991 and then again in July 2013. However, a dramatic increase in seismicity from less than 50 events a day to over 150 events occurred in October 2014, concentrated beneath the summit of Chiles volcano at depths of less than 10 km (Ruiz et al. 2013). Although originally not a target volcano for the VUELCO project, the volcanic complex of Chiles-Cerro Negro is an excellent example of a re-awakening volcano, having shown no signs of magmatic unrest in recent history until the events of 2014. Analysis of seismicity identified in

October 2014 suggested not only the occurrence of families, but also their occurrence in distinct temporal patterns. The clustering of similar seismic events around the diagonal in a number of box-like formations within a similarity matrix suggests that a number of sources were active for discrete periods of time generating families of seismicity (Fig. 5). The distinct clusters of similar seismic waveforms may relate to a changing source location or mechanism at depth (Salvage 2015). Over this time period, no significant changes in the amplitude of events (indicative of a changing source mechanism) were identified. Since similar seismicity is thought to be generated through a similar source mechanism and a similar source location, distinct cluster of similar seismicity is most likely related to its own distinct spatial region, which generated seismicity during distinct periods of time.

## The Source Mechanisms of Low Frequency Earthquakes

Since low frequency events, and in particular families, appear to be important in detecting changes in unrest at volcanoes, it is important to understand their mechanism of generation. Synthetic modelling and moment tensor inversions of low frequency seismic wavefields are powerful tools for gaining information on the source mechanisms underlying volcanic earthquakes. Once instrument response and path effects have been accounted for, real data can be compared to synthetic models, and on the basis of a best-fit approach the obtained model parameters allow insights into the nature and geometry of the source (Chouet 1996; Shuler et al. 2013). However, as the fundamental assumptions behind the commonly used moment tensor inversions are based on plane surface geometries which are believed to be too simple to explain the generation of low frequency events in a volcanic environment, the application to more complex seismic sources has so far been inconclusive. In the framework of the VUELCO project, slip along unbent surfaces (a complex source) was thought of as the underlying physical motion responsible for generating seismic energy. This novel way of investigating low frequency earthquakes can explain several features of the earthquakes under investigation without introducing compromising

assumptions such as slip along a single, unbent surface, which is believed to be unrealistic.

An example of a spatially extended source generating seismicity within a volcanic environment is a volcanic conduit through which magmatic fluids move. In these instances, the generation of low frequency seismicity may be related to the brittle failure of magma itself (Neuberg et al. 2006; Lavallée et al. 2008; Thomas and Neuberg 2012) or through a stick-slip motion at the conduit edge (Iverson et al. 2006). In either case, shallow source depths (1–2 km) and short epicentral distances to seismic receivers (a few kilometers) suggest that a spatially extended source is more realistic than a single point source.

The occurrence of slip (i.e. the generation of the seismic energy itself) of spatially extended sources may either be instantaneous along two or more slip surfaces, or may occur on different slip surfaces at different times, offset by a given time increment,  $\Delta t$ . A ring fault structure is a numerical description of seismogenic slip of magma along all of the conduit walls within a volcanic edifice, and can be numerically modelled by considering a cylinder representing the volcanic conduit with instantaneously slipping double couple (single point) sources bounding the circumference (Fig. 6). Upward movement inside the cylinder and downward movement outside represents the movement of magma

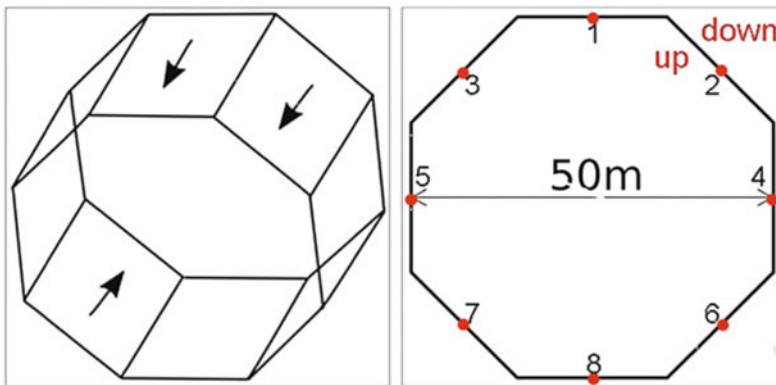


**Fig. 6** Schematic representation of a ring fault structure with movement directed upwards within the cylinder to represent the flow of magma through a conduit. Each

planar surface is host to a single double couple source i.e. a point source (labelled 1–8)

through this channel. Other spatially extended sources which may evoke the generation of low frequency seismicity include: the upward movement of magma through a narrow dyke, numerically modelled by two oppositely directed double couple sources; slip along distinct segments of the volcanic conduit i.e. due to geometry changes (Thomas and Neuberg 2012), numerically modelled with double couple sources on distinct segments; or the generation of a number of seismic swarms of families of earthquakes occurring simultaneously (Salvage and Neuberg 2016), which can be numerically modelled by movement on two or more simultaneously acting ring fault structures.

Green and Neuberg (2006) suggested that accelerated magma movement at Soufrière Hills volcano can be linked to observed deformation cycles through low frequency seismic swarms, and that seismicity is only generated if significant magma movement takes place. Considering slip through extended sources brings us one step closer to estimating magma ascent rates. Once calibrated, the link between observed waveform amplitudes and the amount of seismogenic slip occurring during a seismic swarm will yield magma ascent rates and will ultimately contribute to forecasting volcanic eruptions more accurately. Point and extended source models yield great differences in observed P-wave amplitudes and waveforms, leading to remarkable differences when interpreting the amount of

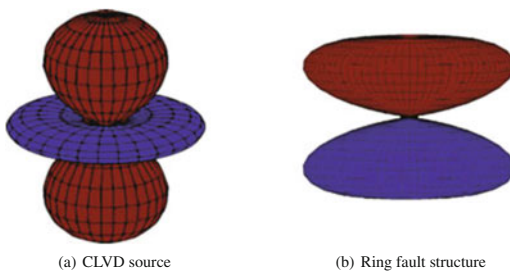


**Fig. 7** P-wave radiation pattern generated for a CLVD source, and for an extended ring fault structure. The *red* lobes are compressional, the *blue* lobes are dilatational. In both radiation patterns a large compressional lobe is found above the source, with dilatational lobes extending radially which can lead to confusion for interpretation of first motion polarity patterns

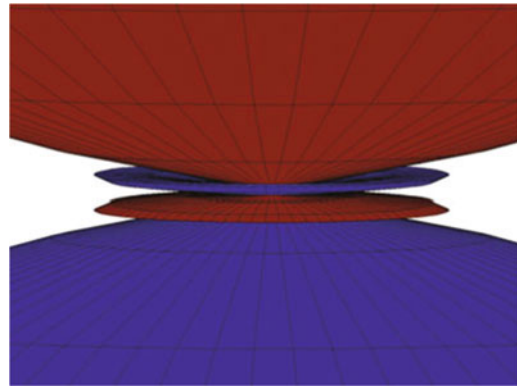


**Fig. 8** Zoom of smaller radial lobes of P-wave radiation pattern for a spatially extended ring fault structure. Compressional lobes are *red*, dilatational lobes are *blue*

slip occurring and the slip rates. In the case of slip along a ring fault, P-wave amplitudes are greatly reduced due to destructive interference, in comparison to simple double couple (point) sources. As a result, observed amplitudes yield an underestimation of actual slip by more than a factor of 3 if interpreted as a point source, when in reality a spatially extended source acts at depth. This underestimation in seismic moment consequently may lead to an underestimation of magma flow rate at depth, which in turn has severe implications for eruption forecasting (Karl 2014).

Furthermore, the P-wave radiation pattern for a spatially extended ring fault structure (i.e. for modelling the movement of magma within the entire conduit made up of a number of double couple sources) shows remarkable similarity to the P-wave radiation pattern for a compensated linear vector dipole (CLVD) source, which instead is a conservation of energy (Fig. 7). The derived ring fault radiation pattern shows rotational symmetry around the depth axis, and consists of a large compressional lobe directly above the source and an inversely polarised, dilatational lobe with the same amplitude below it. Only if the small radial P-wave radiation lobes can be determined for the ring fault structure (Fig. 8) is it possible to distinguish between these two source mechanisms. Seismic networks with small apertures typical in volcanic settings and

uncertainties in earthquake source depth locations will likely lead to difficulties in distinguishing between the two radiation patterns, since both can explain observed first motion polarity patterns of low frequency seismicity on volcanoes (Karl 2014).

## Forecasting Eruptive Activity

The ability to forecast the timing, intensity and type of volcanic activity is one of the key issues facing volcanologists today. The most notable instances of successful volcanic forecasting use precursory activity at andesitic-dacitic volcanoes. The cataclysmic eruption of Mt. Pinatubo, Philippines on 15 June 1991 was preceded by at least two months of heightened seismicity (Harlow et al. 1996). With increases in seismicity and an alarming sudden drop in SO<sub>2</sub>, scientists were able to successfully evacuate over 45,000 local people and 14,500 military personnel to safety by 14 June, such that less than 300 people were killed in the ensuing volcanic activity on 15 June. More recently, the 2010 eruption of Merapi, Indonesia, on 26 September was preceded by approximately 6 weeks of precursory activity (Budi-Santoso et al. 2013): rates of seismicity and SO<sub>2</sub> during this time were comparable to, or higher than, the highest rates observed during previous (smaller) Merapi eruptions (1992–2007), and rapid deformation was observed. Consequently, one day prior to the explosive eruption, several tens of thousands of people were evacuated from a radius extending 10 km from the volcano, resulting in a greatly lowered death toll of 35.

Volcanic eruptions are often preceded by accelerating geophysical signals, associated with the movement of magma or other fluid towards the surface. Of these precursors, seismicity is at the forefront of forecasting volcanic activity since it is frequently observed and the change from background level can be observed in real time. Since forecasting of volcanic eruptions relies on the ability to determine the timing of magma reaching the surface, low frequency seismicity may act as a forecasting tool due to its

potential correlation with the movement of magmatic fluid at depth.

The Failure Forecast Method (FFM) is based on an empirical power-law relationship, which relates the acceleration of a precursor ( $d^2\Omega/dt^2$ ) to the rate of that precursor ( $d\Omega/dt$ ) (Voight 1988) method by:

$$\frac{d^2\Omega}{dt^2} = K \left( \frac{d\Omega}{dt} \right)^\alpha \quad (1)$$

where  $K$  and  $\alpha$  are empirical constants.  $\Omega$  can represent a number of different geophysical precursors, for example low frequency seismic event rate (Salvage and Neuberg 2016), event rate of all recorded seismicity (Kilburn and Voight 1998), or the amplitude of seismic events (Ortiz et al. 2003). The parameter  $\alpha$  is thought to range between 1 and 2 in volcanic environments (Voight 1988), or may even evolve from 1 towards 2 as seismicity proceeds (Kilburn 2003).  $\alpha$  has also been calculated in hindsight as high as 3.3 for accelerating seismicity in 1991 at Mt. Pinatubo, although this extreme value appears rare and was calculated with only a small amount of seismic data (Smith and Kilburn 2010). An infinite  $d\Omega/dt$  suggests an uncontrolled rate of change (a singularity) and in this environment is associated with an impending eruption. The inverse form of  $d\Omega/dt$  is linear if  $\alpha = 2$ , and therefore in this case the solution for the timing of failure is a linear regression of inverse rate against time, with the timing of failure relating to the point where the linear regression intersects the x-axis (Voight 1988).

Although assuming that  $\alpha = 2$  is the simplest method to estimate the timing of an eruption through a linear regression and therefore the most common application of the FFM in hindsight analysis, some authors have suggested that it may not be an appropriate assumption for use with the FFM (e.g. Bell et al. 2011). Additionally, some authors have argued that  $\alpha$  may evolve with time as precursory sequences develop, which is not detailed in the FFM (Kilburn 2003). As the FFM follows a least squares regression analysis when  $\alpha$  is equal to 2, the residual error between the observed event rate and the mean

event rate of seismicity should follow a typical Gaussian distribution (Bell et al. 2011). Greenough and Main (2008) have suggested that since earthquake occurrence is a point process, the rate uncertainties are best described by a Poisson distribution. In this instance, a generalised linear model (GLM) where  $\alpha = 1$ , rather than a least squares regression model ( $\alpha = 2$ ) may be more appropriate, since it can allow for a distribution of data that is non-Gaussian (Bell et al. 2011). At Soufrière Hills volcano, however, the use of a GLM to forecast the timing of eruptive events in 1997 and 2003 failed to generate an appropriate forecast (Salvage and Neuberg 2016). Hammer and Ohrnberger (2012) suggested that this may be related to the fact that a Poisson process, and therefore the GLM, is a memoryless system, meaning that past events do not influence future patterns. A memoryless system is not consistent with the fundamental assumptions of the FFM, since previous geophysical observables form the basis of such a forecast.

One of the first instances of real time forecasting using the FFM was at Redoubt volcano, when the inverse average amplitude of seismic

events followed a linear regression trend for 4 days prior to a dome collapse event on 2 January 1990. Due to this trend, and the fact that the seismic intensity was far above background levels, the Alaskan Volcano Observatory issued a “formal warning” of an impending eruptive event on the morning of the 2 January, a few hours before the eruption began, although the FFM calculations suggested an eruption was likely within 0.5–2 days. A similar, if not clearer trend, that supported the forecast was found using the same precursory sequence but only using seismic events within the spectral range of 1.3–1.9 Hz (Cornelius and Voight 1994), suggesting an increased accuracy in forecasts when focusing on a single source process at depth.

Swarms of seismic events, i.e. a number of similar events within a short period of time, with typical swarm durations of hours to day, are not observed at all volcanoes, but have been commonly observed at Soufrière Hills volcano (e.g. Green and Neuberg 2006) and Redoubt volcano (e.g. Buurman et al. 2013). Using precursory seismicity and the FFM, Salvage and Neuberg (2016) forecast in hindsight the timing of a dome collapse event on 25 June 1997 at Soufrière

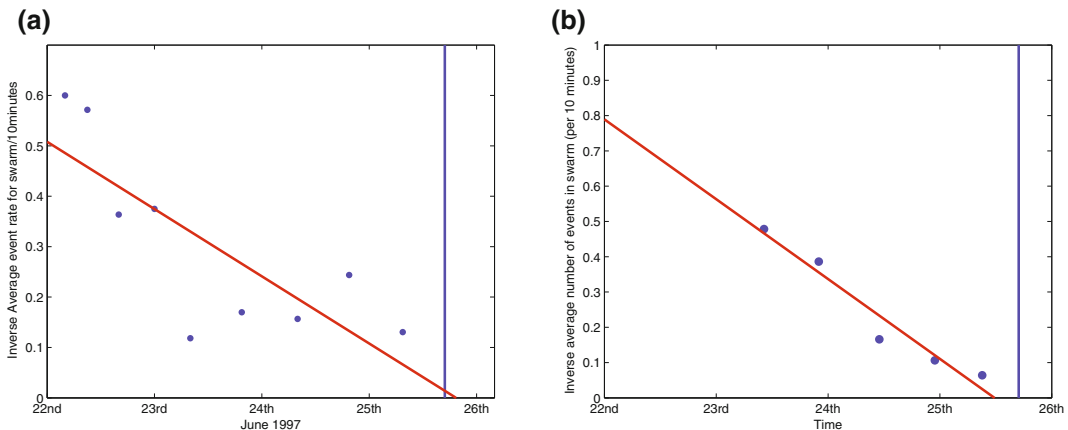


**Fig. 9** Application of the FFM: the inverse average event rate per 10 min within swarms from 22 to 25 June 1997 at a single station at Soufrière Hills volcano. Each data point represents the inverse average event rate for each individual identified swarm of seismicity. The vertical line represents the known timing of dome collapse on the 25 June 1997 at 16:55 UTC. The

graphical representation of the FFM is depicted by the linear regression (it is assumed that  $\alpha = 2$  for simplicity) and the forecasted timing of failure can be read off the x-axis at the point where the linear regression crosses it. **a** All triggered low frequency seismicity. **b** Single family of similar seismicity



Hills, based upon accelerating rates of low frequency earthquakes which occurred in swarms, rather than simply the number of low frequency events over the precursory time period (Fig. 9). Using the average event rate per swarm showed a clearer accelerating pattern over the entire seismic sequence, rather than using the traditional method of binning data in units of time. More accurate forecasts were determined when using only one single family of similar events to forecast the dome collapse, rather than all low frequency seismicity mixed together. A dome collapse on 12 July 2003 at Soufrière Hills volcano was also more accurately forecast when using a single family of similar events, rather than all low frequency seismicity, which occurred during the period of unrest (Salvage and Neuberg 2016). Consequently, the use of families of seismicity, and therefore concentration upon a single active system at depth, may allow a more accurate forecast of the timing of an eruptive event in these instances.

---

## Summary

Seismology is a powerful tool which can be used to understand processes occurring at depth, and their relationship to the surface at volcanoes, especially since seismic events are easily detected and the deviation from the background level is often notably pronounced. An increase in seismicity may be an indication of volcanic unrest, since it relates to a number of physical processes at depth including brittle failure and fracturing of the conduit or of the surrounding edifice (high frequency seismicity) and the movement of magmatic fluids at depth (low frequency seismicity). Using families of seismicity as an indicator of a single active system at depth, temporal and spatial patterns in the seismic events can be used to assess the potential migration of seismicity towards the surface, as well as to forecast the timing of volcanic eruptive events related to the acceleration of seismicity. However, a full understanding of the source mechanism of the generated seismic events is

essential to ensure that the magma flow rate is estimated accurately and therefore an accurate forecast can be generated for the timing of eruption. Using seismicity in combination with other monitoring tools, we are now closer to gaining a better understanding of evolving magmatic systems at depth.

**Acknowledgements** The past and present staff at the Montserrat Volcano observatory are fully acknowledged for their ongoing support in the upkeep and maintenance of the seismic network, and the sharing of data. All staff at the Instituto-Geofísico in Ecuador are also fully acknowledged for providing data from Chiles-Cerro Negro volcano, for useful discussions regarding the volcanic complex, and for their continued monitoring efforts of all volcanoes in Ecuador. We thank two anonymous reviewers for their detailed comments and suggestions which greatly enhanced the quality of this manuscript. Muchas gracias también a Maria Martinez-Cruz y Javier Pacheco por su ayuda con la traducción al español.

---

## References

- Arámbula-Mendoza R, Lesage P, Valdés-González C, Varley N, Reyes-Dávila G, Navarro C (2011) Seismic activity that accompanied the effusive and explosive eruptions during the 2004–2005 period at Volcán de Colima, Mexico. *J Volcanol Geoth Res* 205(1):30–46
- Arciniega-Ceballos A, Chouet B, Dawson P (2003) Long-period events and tremor at Popocatepetl volcano (1994–2000) and their broadband characteristics. *Bull Volc* 65(2):124–135
- Bean CJ, De Barros L, Lokmer I, Métaixian J-P, O'Brien G, Murphy S (2014) Long-period seismicity in the shallow volcanic edifice formed from slow-rupture earthquakes. *Nat Geosci* 7(1):71–75
- Beauval C, Yepes H, Bakun WH, Egred J, Alvarado A, Singaicho J-C (2010) Locations and magnitudes of historical earthquakes in the Sierra de Ecuador (1587–1996). *Geophys J Int* 181(3):1613–1633
- Bell A, Naylor M, Heap M, Main I (2011) Forecasting volcanic eruptions and other material failure phenomena: an evaluation of the failure forecast method. *Geophys Res Lett* 38:L15304
- Budi-Santoso A, Lesage P, Dwiyono S, Sumarti S, Jousset P, Métaixian J-P et al (2013) Analysis of the seismic activity associated with the 2010 eruption of Merapi Volcano, Java. *J Volcanol Geoth Res* 261:153–170
- Budi-Santoso A, Lesage P (2016) Velocity variations associated with the large 2010 eruption of Merapi volcano, Java, retrieved from seismic multiplets and ambient noise cross-correlation. *Geophys J Int* 206(1):221–240

- Buurman H, West ME, Thompson G (2013) The seismicity of the 2009 Redoubt eruption. *J Volcanol Geoth Res* 259:16–30
- Chouet B (1988) Resonance of a fluid-driven crack: radiation properties and implications for the source of long-period events and harmonic tremor. *J Geophys Res Solid Earth* (1978–2012) 93(B5), 4375–4400
- Chouet BA (1996) New methods and future trends in seismological volcano monitoring. In: *Monitoring and Mitigation of Volcano Hazards*. Springer, pp. 23–97
- Chouet BA, Matoza RS (2013) A multi-decadal view of seismic methods for detecting precursors of magma movement and eruption. *J Volcanol Geoth Res* 252:108–175
- Cornelius R, Voight B (1994) Seismological aspects of the 1989–1990 eruption at Redoubt Volcano, Alaska: the materials Failure Forecast Method (FFM) with RSAM and SSAM seismic data. *J Volcanol Geoth Res* 62(1):469–498
- Dawson PB, Chouet BA, Power J (2011) Determining the seismic source mechanism and location for an explosive eruption with limited observational data: Augustine Volcano, Alaska. *Geophys Res Lett* 38(3):L03302
- De Angelis S, Henton S (2011) On the feasibility of magma fracture within volcanic conduits: constraints from earthquake data and empirical modelling of magma viscosity. *Geophys Res Lett* 38(19):L19310
- De Angelis S, Bass V, Hards V, Ryan G (2007) Seismic characterization of pyroclastic flow activity at Soufrière Hills Volcano, Montserrat, 8 January 2007. *Nat Hazards Earth Syst Sci* 7:467–472
- Geller R, Mueller C (1980) Four similar earthquakes in central California. *Geophys Res Lett* 7(10):821–824
- Goto A (1999) A new model for volcanic earthquake at unzen volcano: melt rupture model. *Geophys Res Lett* 26(16):2541–2544
- Green D, Neuberg J (2006) Waveform classification of volcanic low-frequency earthquake swarms and its implication at Soufrière Hills Volcano, Montserrat. *J Volcanol Geoth Res* 153(1):51–63
- Greenhough J, Main I (2008) A poisson model for earthquake frequency uncertainties in seismic hazard analysis. *Geophys Res Lett* 35(19):L19313
- Hammer C, Ohrnberger M (2012) Forecasting seismo-volcanic activity by using the dynamical behavior of volcanic earthquake rates. *J Volcanol Geoth Res* 229:34–43
- Harlow DH, Power JA, Laguerta EP, Ambubuyog G, White RA, Hoblitt RP (1996) Precursory seismicity and forecasting of the June 15, 1991, eruption of Mount Pinatubo. *Eruptions and lahars of Mount Pinatubo, Philippines, Fire and mud*, pp 223–247
- Herd RA, Edmonds M, Bass VA (2005) Catastrophic lava dome failure at Soufrière Hills volcano, Montserrat, 12–13 July 2003. *J Volcanol Geoth Res* 148(3):234–252
- Iverson R, Dzurisin D, Gardner C, Gerlach T, LaHusen R, Lisowski M, Major J, Malone S, Messerich J, Moran S et al (2006) Dynamics of seismogenic volcanic extrusion at Mount St Helens in 2004–05. *Nature* 444(7118):439–443
- Karl S (2014) The source mechanisms of low frequency seismic events on volcanoes. Ph.D. thesis, University of Leeds, UK, Online at: <http://etheses.whiterose.ac.uk/id/eprint/8406>
- Kilburn C (2003) Multiscale fracturing as a key to forecasting volcanic eruptions. *J Volcanol Geoth Res* 125(3–4):271–289
- Kilburn CR, Voight B (1998) Slow rock fracture as eruption precursor at Soufrière Hills volcano Montserrat. *Geophys Res Lett* 25(19):3665–3668
- Lahr J, Chouet B, Stephens C, Power J, Page R (1994) Earthquake classification, location, and error analysis in a volcanic environment: implications for the magmatic system of the 1989–1990 eruptions at Redoubt Volcano, Alaska. *J Volcanol Geoth Res* 62(1):137–151
- Lavallée Y, Meredith P, Dingwell D, Hess K-U, Wassermann J, Cordonnier B, Gerik A, Kruhl J (2008) Seismogenic lavas and explosive eruption forecasting. *Nature* 453(7194):507–510
- McNutt SR (2005) Volcanic seismology. *Annu Rev Earth Planet Sci* 32:461–491
- Nakano M, Kumagai H (2005) Response of a hydrothermal system to magmatic heat inferred from temporal variations in the complex frequencies of long-period events at Kusatsu-Shirane Volcano, Japan. *J Volcanol Geoth Res* 147(3):233–244
- Neuberg J, Luckett R, Baptie B, Olsen K (2000) Models of tremor and low-frequency earthquake swarms on Montserrat. *J Volcanol Geoth Res* 101(1–2):83–104
- Neuberg J, Tuffen H, Collier L, Green D, Powell T, Dingwell D (2006) The trigger mechanism of low-frequency earthquakes on Montserrat. *J Volcanol Geoth Res* 153(1):37–50
- Ortiz R, Moreno H, Garcà A, Fuentealba G, Astiz M, Peña P, Sánchez N, Tárraga M (2003) Villarrica volcano (Chile): characteristics of the volcanic tremor and forecasting of small explosions by means of a material failure method. *J Volcanol Geoth Res* 128(1):247–259
- Ottmøller L (2008) Seismic hybrid swarm precursory to a major lava dome collapse: 9–12 July 2003, Soufrière Hills Volcano, Montserrat. *J Volcanol Geoth Res* 177(4):903–910
- Petersen T (2007) Swarms of repeating long-period earthquakes at Shishaldin Volcano, Alaska, 2001–2004. *J Volcanol Geoth Res* 166(3):177–192
- Phillipson G, Sobradelo R, Gottsmann J (2013) Global volcanic unrest in the 21st century: an analysis of the first decade. *J Volcanol Geoth Res* 264:183–196
- Ruiz G, Cordova A, Ruiz M, Alvarado A (2013) Informe Técnico de los volcanes Cerro Negro y Chiles. Tech. Rep., IG-EPN, in Spanish
- Salvage RO (2015) Using seismic signals to forecast volcanic processes. Ph.D. thesis, University of Leeds, UK, Online at: <http://etheses.whiterose.ac.uk/12268/>. Restricted until April 2018
- Salvage R, Neuberg J (2016) Using a cross correlation technique to refine the accuracy of the failure forecast method: application to Soufrière Hills volcano, Montserrat. *J Volcanol Geoth Res* 324:118–133



- Sgattoni G, Jeddi Z, Gudmundsson Ó, Einarsson P, Tryggvason A, Lund B, Lucchi F (2016) Long-period seismic events with strikingly regular temporal patterns on Katla volcano's south flank (Iceland). *J Volcanol Geoth Res* 324:28–40
- Shuler A, Ekström G, Nettles M (2013) Physical mechanisms for vertical-CLVD earthquakes at active volcanoes. *J Geophys Res Solid Earth* 118(4):1569–1586
- Smith R, Kilburn C (2010) Forecasting eruptions after long repose intervals from accelerating rates of rock fracture: the June 1991 eruption of Mount Pinatubo, Philippines. *J Volcanol Geoth Res* 191(1):129–136
- Sparks R, Young S (2002) The eruption of Soufrière Hills Volcano, Montserrat (1995–1999): overview of scientific results. *Geol Soc Lond Mem* 21(1):45–69
- Thelen W, Malone S, West M (2011) Multiplets: their behavior and utility at dacitic and andesitic volcanic centers. *J Geophys Res Solid Earth* (1978–2012) 116 (B8):B08210
- Thomas ME, Neuberg J (2012) What makes a volcano tick—a first explanation of deep multiple seismic sources in ascending magma. *Geology* 40(4):351–354
- Voight B (1988) A method for prediction of volcanic eruptions. *Nature* 332:125–130
- Wadge G, Voight B, Sparks R, Cole P, Loughlin S, Robertson R (2014) An overview of the eruption of Soufriere Hills Volcano, Montserrat from 2000 to 2010. Geological Society, London, *Memoirs* 39(1):1–40

**Open Access** This chapter is licensed under the terms of the Creative Commons Attribution 4.0 International License (<http://creativecommons.org/licenses/by/4.0/>), which permits use, sharing, adaptation, distribution and reproduction in any medium or format, as long as you give appropriate credit to the original author(s) and the source, provide a link to the Creative Commons license and indicate if changes were made.

The images or other third party material in this chapter are included in the chapter's Creative Commons license, unless indicated otherwise in a credit line to the material. If material is not included in the chapter's Creative Commons license and your intended use is not permitted by statutory regulation or exceeds the permitted use, you will need to obtain permission directly from the copyright holder.

